JOURNAL OF MATERIALS SCIENCE 26 (1991) 2343–2347

Effect of double-ageing on mechanical properties of Mg–6Zn reinforced with SiC particulates

P. K. CHAUDHURY, H. J. RACK
Department of Mechanical Engineering, Clemson University, Clemson, SC 29634, USA
B. A. MIKUCKI
The Dow Chemical Company, Lake Jackson Research Center, Freeport, TX, USA

Double-age hardening characteristics of a Mg–6% Zn alloy reinforced with 20 vol% SiC particulates (SiC_p) were examined. Tensile tests were conducted using specimens with two different double-ageing treatments. Examination of the fracture surface using scanning electron microscopy and energy dispersive analysis of X-rays, and study of the precipitation process using transmission electron microscopy were undertaken to supplement the mechanical test data. The results show pre-ageing below the Guinier–Preston zone solvus strengthens the matrix through refinement of precipitates, and in turn leads to an increase in strength and decrease in composite ductility. In addition, as the yield and ultimate tensile strength of the composite increase, involvement of SiC_p in the fracture process increases.

1. Introduction

Increasing demands for material with higher specific strengths and stiffnesses have resulted in the development of lightweight metal-matrix composites. While most studies have been focused on aluminium metal-matrix composites, magnesium, with suitable alloying and reinforcement, has shown increasing potential in many applications [1, 2]. Magnesium alloys reinforced with SiC particulates (SiC_p) possess the following attractive features.

(i) SiC particles are relatively inexpensive and can be successfully introduced by low-cost liquid metallurgy techniques [3].

(ii) Conventional fabrication/shaping can be used.

(iii) Mechanical properties of the matrix can be dramatically improved via alloying and thermo-mechanical treatments, e.g. Mg–Zn alloys with 4%–8 wt % Zn are capable of age hardening [4–11].

While the age-hardening behaviour of discontinuously reinforced aluminium alloy matrix composites has been investigated extensively [12–19] such efforts using Mg alloy matrix composite are very limited [20]. The present investigation considered the potential for increasing the mechanical performance of a cast and extruded Mg–6% Zn matrix reinforced with SiC particulates utilizing a double ageing technique. Mechanical properties, e.g. modulus of elasticity, yield strength, ultimate tensile strength and ductility are evaluated, and correlated with microstructural and fracture surface examinations.

2. Experimental procedure

The material used in this investigation, an ingot-processed Mg–6Zn–0.3Ca alloy reinforced with 20 vol % SiC particulate, was prepared at Dow Chemical Corporation, Lake Jackson, Texas. The reinforcement was introduced by a proprietory liquid metallurgy technique developed at Dow utilizing 1000 grit, nominally 8–10 μm diameter, SiC particulate containing approximately 1% free carbon [3]. The composite material was then cast into an ingot, 63.5 cm long and 17.8 cm diameter, and extruded to a 6.35 cm diameter bar.

Cylindrical tensile specimens with gauge length and diameter of 2.54 and 0.635 cm, respectively, were machined from the bar. All specimens were solution treated at 673 K for 4 h in a protective atmosphere of argon gas and water quenched. Finally, the specimens were double aged according to the following schedule.

Heat treatment 1: artificial ageing at 343 K for 24 h followed by 423 K for 48 h.
Heat treatment 2: artificial ageing at 353 K for 24 h followed by 423 K for 48 h.

Room-temperature tensile tests were conducted on double aged specimens on an Instron servo-hydraulic machine at a strain rate of 0.01 min^{-1}. For each ageing schedule 9–12 tests were conducted and elastic modulus, yield strength, ultimate tensile strength and ductility were recorded. Fracture surfaces of selected specimens were examined using a Jeol 848 scanning electron microscope equipped with a Tracor Northern X-ray analyser.

Finally, differences in precipitate substructure resulting from the two ageing schedules were studied by transmission electron microscopy. Thin foils were prepared for examination utilizing a Jeol 100C transmission electron microscope operated at 100 kV by diamond sectioning, hand grinding to a 75 μm thick disc

0022–2461/91 $03.00 + .12

TABLE I Tensile properties of 20 vol % SiC_p/Mg–6Zn

Double-ageing condition	E (GPa)	S_y (MPa)	S_u (MPa)	e_f (%)	
				Total	Plastic
1. 343 K/24 h + 423 K/48 h	75.9	411	467	2.9	2.3
2. 353 K/24 h + 423 K/48 h	77.2	348	425	4.9	4.3

and argon ion milling at 6 kV, 0.4 mA and a 15° impingement angle.

3. Results

Tensile test results are summarized in Table I where elastic modulus, E, yield strength, S_y, ultimate tensile strength, S_u, and fracture strain, e_f, both plastic and total, are tabulated for the two double-ageing conditions. Comparison of these results with those normally observed in commercial wrought alloys, e.g. ZE63A in the T6 temper, $E = 45$ GPa, $S_y = 190$ MPa, $S_u = 300$ MPa and $e_f = 10\%$ [21], show large improvements in elastic modulus and strength properties; however, these improvements are associated with a considerable decrease in ductility. Similar behaviour has been observed in SiC-reinforced aluminium matrix composites [22–24] where age hardening of the matrix is associated with an increase in composite strength and a decrease in ductility.

Further, the yield strength and ultimate tensile strength decreased significantly as the pre-ageing temperature was increased from 343 K (heat treatment 1) to 353 K (heat treatment 2). Similar heat treatments for unreinforced binary Mg–6Zn (solution treatment, water quench + 96 h at 338 K + 16 h at 443 K) and ternary Mg–6Zn–1Au (solution treatment, water quench + 24 h at 363 K + 16 h at 443 K) alloys have shown the benefits of low-temperature pre-ageing [6].

The transmission electron microscopy results are presented in Figs 1 and 2. In specimens pre-aged at 343 K two types of closely-spaced and orthogonally-oriented, rod-like precipitates predominated, Fig. 1. In contrast, pre-ageing at 353 K resulted in the formation of a mixture of large globular, Fig. 2a, and very fine and unidirectional rod-like precipitates, Fig. 2b. Precipitates with similar morphologies have been observed in several studies and are characteristic of precipitation in unreinforced Mg–Zn (4%–8%) alloys [4–10]. The globular precipitates are the equilibrium MgZn phase, the long rod-like precipitates, which grow along the c-axis of the matrix are transition β'_1 phase, Figs 1 and 2b, while the comparatively shorter rods perpendicular to the β'_1 precipitates are another transition phase, β'_2, Fig. 1.

Results of the fracture surface examination are presented in Figs 3–6. SiC particle clumps, especially close to the tensile sample surface, serve as sites for fracture initiation. Fig. 3 shows such an example where scanning electron micrographs, at low, Fig. 3a, and high, Fig. 3b, magnifications, as well as energy dispersive spectrum, Fig. 3c, for this area are presented. In addition, evidence exists that Ca-containing inclusions, Fig. 4, may also contribute to fracture initiation.

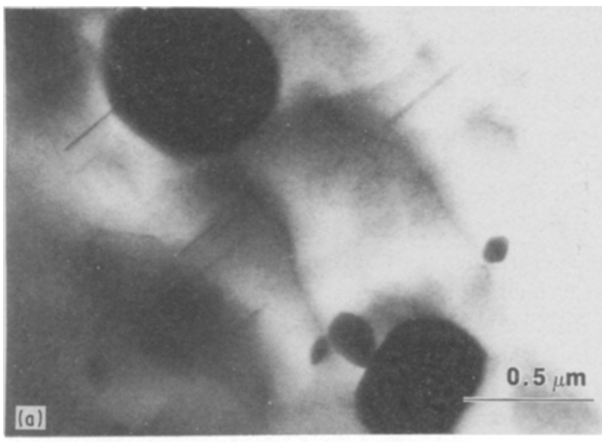

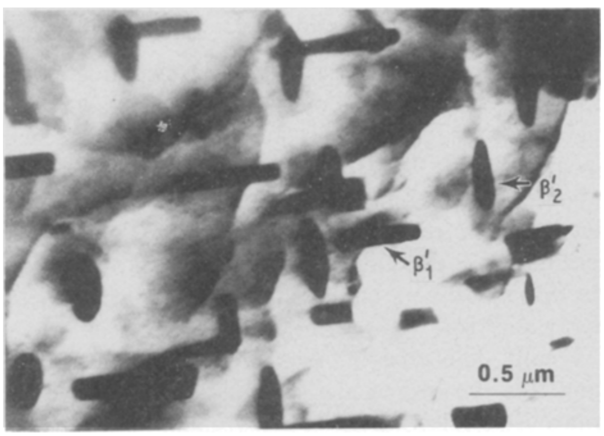

Figure 1 Transmission electron micrograph of 20 vol % SiC_p/Mg–6Zn composite double-aged at 343 K/24 h + 423 K/48 h, showing precipitation of β'_1 and β'_2.

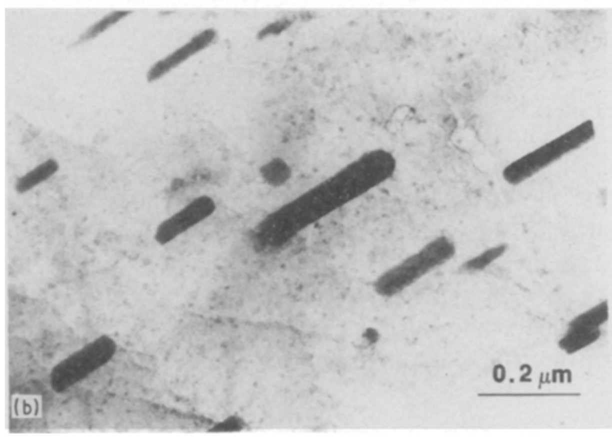

Figure 2 Transmission electron micrograph of 20 vol % SiC_p/Mg–6Zn composite double-aged at 353 K/24 h + 423 K/48 h, showing (a) large β precipitates and (b) fine β_1 precipitates.

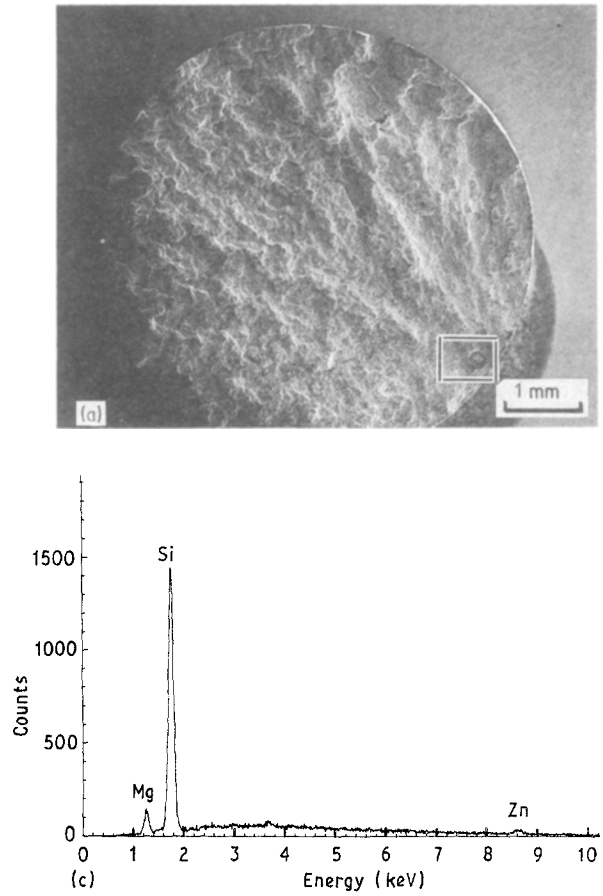

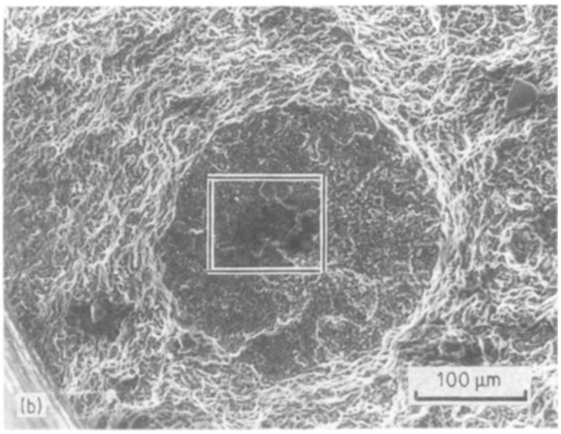

Figure 3 Scanning electron micrograph and EDX spectrum of tensile fracture surface of double-aged 20 vol % SiC_p/Mg–6Zn composite, showing fracture initiation at SiC_p-rich area: (a) fracture surface at low magnification; (b) fracture initiation site as boxed in (a); and (c) EDX spectrum of the boxed area in (b), showing SiC_p segregation at the fracture initiation site.

However, once initiated, the fracture mode for both ageing conditions consists of a bimodal distribution of large dimples, typically associated with SiC particulates, and smaller dimples, Fig. 5.

Further study indicates that the fracture path is dependent on ageing practice. Quantitative analysis, utilizing Si mapping, indicates that the total amount of exposed SiC on the fracture surface was 20.4 $\pm$ 2 vol % and 14.7 $\pm$ 3 vol % in specimens pre-aged at 343 and 353 K, respectively, Fig. 6.

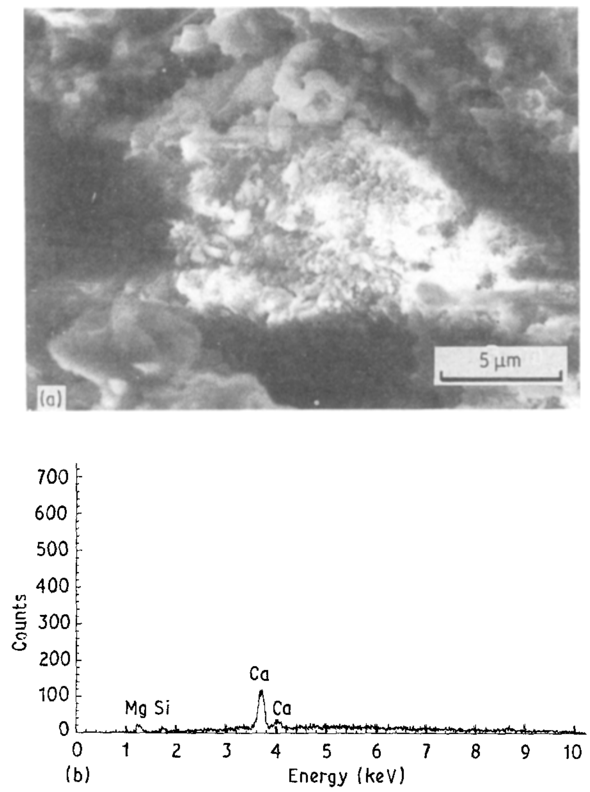

Figure 4 (a) Scanning electron micrograph, and (b) EDX spectrum, of tensile fracture surface of double-aged 20 vol % SiC_p/Mg–6Zn composite, showing Ca-rich inclusion.

4. Discussion

A recent study of the age-hardening response of Mg–6Zn reinforced with SiC_p showed [20] that the

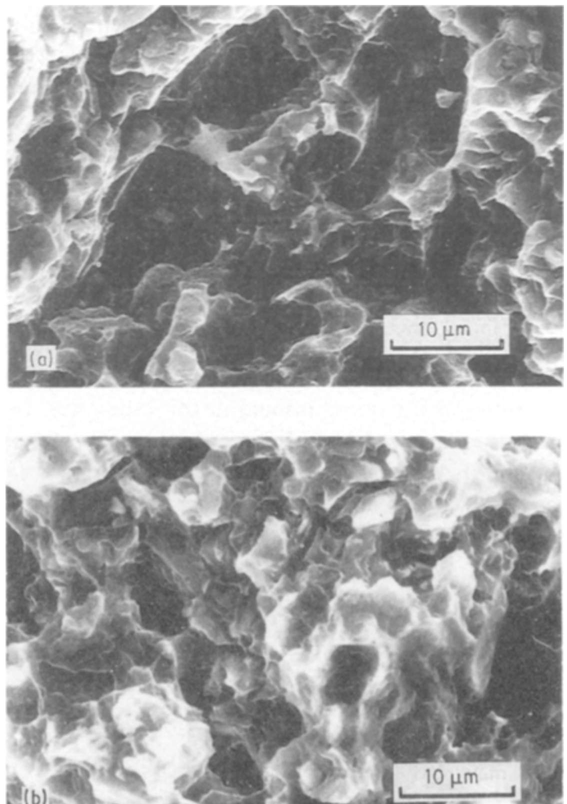

Figure 5 Scanning electron micrographs of tensile fracture surface of double-aged 20 vol % SiC_p/Mg–6Zn composites, showing bimodal distribution of large and small dimples under double-ageing conditions: (a) 343 K/24 h + 423 K/48 h and (b) 353 K/24 h + 423 K/48 h.

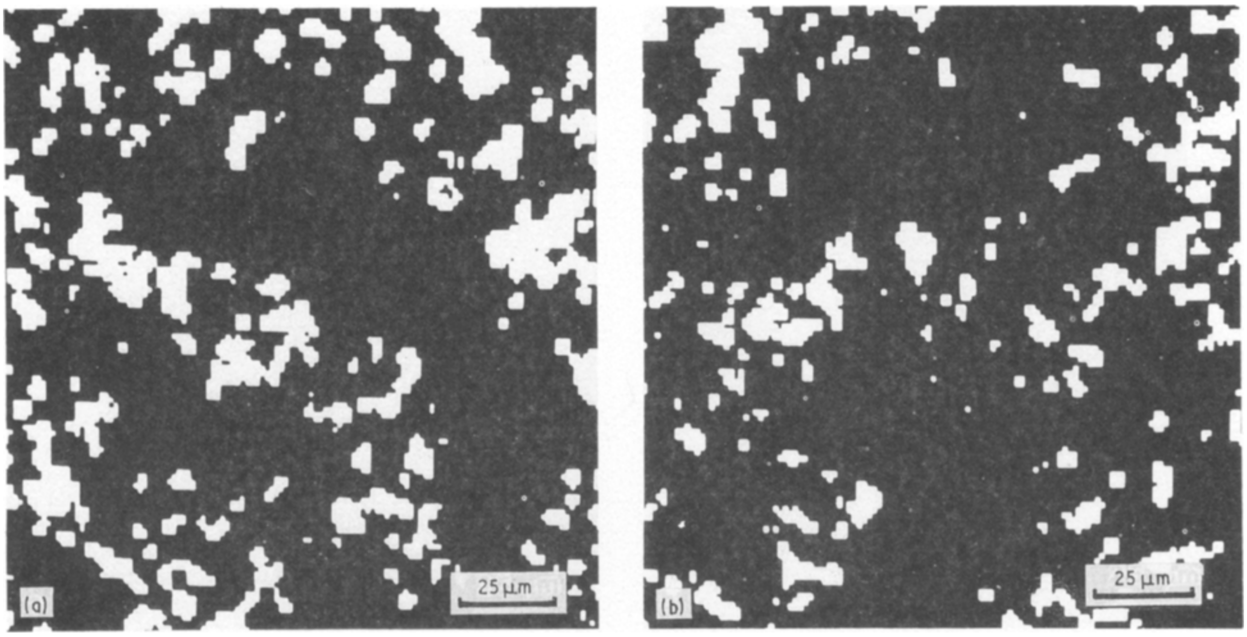

Figure 6 Si mapping on fracture surface showing amount of exposed SiC_p on tensile fracture surface of 20 vol % SiC_p/Mg–6Zn composites under double-ageing conditions of (a) 343 K/24 h + 423 K/48 h and (b) 353 K/24 h + 423 K/48 h.

ageing sequence in the composite is similar to that observed in the unreinforced alloy, i.e.

$$\text{SSS} \rightarrow \text{Guinier–Preston zones} \rightarrow \beta' \rightarrow \beta' \text{ (MgZn)} \quad (1)$$

While β is the equilibrium phase with a globular morphology, β' is a long and rod-like stable transition phase which is responsible for strengthening at peak-aged condition. β' has two morphological variables: β'_1 and β'_2, both having a structure of Laves $MgZn_2$ type [6, 7]. The former variation has been observed to nucleate heterogeneously and grow parallel to the c-axis of the matrix, while the latter has been observed to precipitate at longer times and/or higher temperatures with an orientation orthogonal to β'_1 precipitates. The reported [6] lattice parameters and matrix–precipitate orientation relationships of β'_1 and β'_2 suggest that the delayed precipitation of β'_2 is due to the difference in interfacial strain energy resulting from the anisotropic nature of the Mg matrix [25, 26].

Double-ageing, as examined in this study, has been successfully applied to a wide range of age-hardenable aluminium alloys [26, 27]. In these alloys it normally consists of pre-ageing at low temperature, typically below the Guinier–Preston (GP) zone solvus, followed by ageing at higher temperatures. The pre-ageing treatment is designed to provide a uniformly distributed array of GP zones which can serve as subsequent sites for nucleation, and thereby facilitate homogeneous distribution of the hardening phase. It is well known that this treatment is particularly beneficial when the strain fields associated with the intermediate phases are large, in such cases precipitates of these intermediate phases are sensitive to lattice imperfections.

Present results, including tensile properties and TEM observations, have demonstrated that similar benefits may be achieved in age hardenable Mg–Zn composites. Overall response of the double-aged SiC_p-reinforced Mg–6Zn composite may be explained in terms of the existence of a metastable GP zone solvus at approximately 348 K, as reported for binary Mg–6Zn [6]. Pre-ageing below this temperature, i.e. at 343 K, prior to ageing at 423 K results in a refined microstructure, and improved yield and ultimate tensile strengths. On the other hand, pre-ageing at higher temperature, 353 K, i.e. above the solvus, followed by ageing at 423 K leads to precipitation of coarser β.

This double ageing treatment when applied to SiC_p-reinforced Mg–Zn composites can result in specific modulus and strength properties, which are comparable, and in some cases superior to, those achievable in either standard aluminium or reinforced aluminium alloys, Table II.

Further, this study has shown that the tensile fracture initiation, of current SiC_p-reinforced Mg–Zn composites is controlled by (a) the presence of tramp inclusions, and (b) the uniformity of SiC_p dispersion. Large Ca-rich inclusions, together with non-uniformly distributed SiC_p clumps, serve as the initial site for failure initiation. Similar observations have been reported in early SiC_p-reinforced aluminium alloys [29], subsequent processing modifications having largely eliminated this source of premature failure.

Finally, the ductility of SiC_p-reinforced Mg–Zn alloys is limited by the ability of the matrix to redistribute stress concentration through plastic flow. For example, when these composites were pre-aged at 353 K, quantitative analysis of the fracture surface indicated that the fracture path was matrix dominated, that is the volume per cent SiC_p on the fracture surface, 14.7%, was less than that of the overall composite. However, when the ageing treatment involved pre-ageing at 343 K, higher matrix flow properties were achieved, and the volume per cent SiC_p present on the fracture surface increased to that of the overall composite. These observations are consistent with accumulating evidence in SiC_p-reinforced aluminium

TABLE II Comparison of specific modulus and strength of 20 vol % SiC_p/Mg-6Zn with other materials

Material	Condition	Sp. E ($kN m g^{-1}$)	Sp. S_y ($N m g^{-1}$)	Sp. S_u ($N m g^{-1}$)
20 vol %	Double-aged			
	1[a]	36.1	195.7	222.4
SiC_p/Mg-6Zn	2[a]	36.8	165.7	202.3
7050 Al	peak-aged			
Forging [20]	at 373 K	24.8	185.0	185.0
7475 Al	peak-aged			
T61 [20]	at 373 K	24.8	182.3	201.8
20% SiC_p/2124 Al [28]	peak-aged	36.2	140.0	193.1
20% SiC_p/6061 Al [28]	peak-aged	36.9	147.8	177.3
20% SiC_p/7090 Al [28]	peak-aged	35.9	225.8	249.6

[a] Heat-treatment number.

alloys; tensile failure of lower strength 2124/SiC_p composites occurs randomly [30], while failure in higher strength 7xxx/SiC_p composites is dominated by the presence of the SiC_p [31].

5. Conclusions

1. Elastic modulus, yield strength and ultimate tensile strength of double-aged Mg–Zn reinforced with 20 vol % SiC particulates are higher than conventional age-hardened Mg–Zn alloys. Specific strengths and modulus are comparable to high-strength Al alloys and many SiC/Al composites.

2. Lower pre-ageing temperatures result in higher yield and ultimate tensile strengths with some decrease in ductility.

3. Tensile failure is initiated at large SiC_p-rich or Ca-rich areas.

4. The higher strengths are due to refinement of precipitates in the microstructure, while the loss of ductility is caused by the increased failure associated with SiC particulates.

Acknowledgement

Two of the authors, PKC and HJR, thank the US Air Force Office of Scientific Research, contract F49620-C-0017, for financial support as part of the University Research Initiative programme on High Temperature Metal Matrix Composites at Carnegie Mellon University.

References

1. Proceedings of the 44th Annual World Magnesium Conference, Tokyo, Japan, 17–20 May 1987, International Magnesium Association McLean, VA, USA.
2. S. J. SWINDLEHURST and I. W. HALL, in "Proceedings of the International Symposium on Advances in Cast Reinforced Metal Composites", edited by S. G. Fishman and A. K. Dhingra (ASM International, Metals Park, Ohio, 1988) p. 281.
3. B. A. MIKUCKI, S. C. SHOOK, W. E. MERCER II and W. G. GREEN, *Light Metal Age* **44** (1986) 16.
4. L. STURKEY and J. B. CLARK, *J. Inst. Metals* **88** (1959–60) 177.
5. J. B. CLARK, *Acta Metall.* **13** (1965) 1281.
6. E. O. HALL, *J. Inst. Metals* **96** (1968) 21.
7. M. BERNOLE, J. GALLOT and R. GRAF, *J. Microscopie* **4** (1965) 787.
8. G. MIMA and Y. TANAKA, *Nippon Kinzoku Gakkaishi* **33** (1969) 796.
9. J. S. CHUN, J. G. BYRNE and A. BORNEMANN, *Phil. Mag.* **20** (1969) 291.
10. G. MIMA and Y. TANAKA, *Nippon Kinzoku Gakkaishi* **34** (1970) 209.
11. G. MIMA and Y. TANAKA, *Trans. JIM* **12** (1971) 323.
12. H. J. RACK, in "Powder Metallurgy Composites", edited by P. Kumar, K. Vedula and A. Ritter (The Metallurgical Society, Warrendale, PA, 1988) p. 155.
13. H. J. RACK, in "Dispersion Strengthen Aluminium Alloys", edited by Y.-W. Kim (The Metallurgical Society, Warrendale, PA, 1988) p. 649.
14. T. CHRISTMAN and S. SURESH, *Acta Metall.* **36** (1988) 1691.
15. R. J. ARSENAULT and S. B. WU, *Scripta Metall.* **22** (1988) 767.
16. J. M. PAPAZIAN, *Met. Trans.* **19A** (1988) 2945.
17. H. J. RACK, in "Proceedings of ICCM-VI", Vol. 2, edited by F. L. Mathews, N. C. R. Buskell, J. M. Hodgkinson and J. M. Morton (Elsevier Applied Science, London, 1987) p. 382.
18. S. NUTT and R. W. CARPENTER, *Mater. Sci. Engng* **75** (1985) 169.
19. T. G. NEIH and R. F. KARLAK, *Scripta Metall* **18** (1984) 25.
20. H. J. RACK and P. K. CHAUDHURY, in "Light-Weight Alloys for Aerospace Applications", edited by E. W. Lee, E. H. Chia and N. J. Kim (The Minerals, Metals and Materials Society, Warrendale, PA, 1989) p. 345.
21. "Metals Handbook" (ASM International, Metals Park, Ohio, 1979) p. 592, 9th Edn, Vol. 2.
22. T. G. NIEH, R. A. RAINEN and D. J. CHELLMAN, in "Proceedings of ICCM-V", edited by W. C. Harrigan Jr, J. Strife and A. K. Dhingra (1985) p. 825.
23. C. R. CROWE, R. A. GRAY and D. F. HASSON, *ibid.*, p. 843.
24. D. McDANELS, *Met. Trans.* **16A** (1985) 1105.
25. J. K. LEE, D. M. BARNETT and H. I. AARONSON, *ibid.* **8A** (1977) 963.
26. P. E. MARTH, H. I. AARONSON, G. W. LORIMER, T. L. BARTEL and K. C. RUSSELL, *ibid.* **7A** (1976) 1519.
27. H. LOFTLER, I. KOVACS and J. LENDVAI, *J. Mater. Sci.* **18** (1983) 2215.
28. W. C. HARRIGAN Jr, in "Engineered Materials Handbook" (ASM International, Metals Park, Ohio, 1987) Vol. 1, p. 893.
29. J. W. MULLENS and H. J. RACK, in "High Strength Powder Metallurgy Aluminium Alloys II", edited by G. J. Hildeman and M. J. Koczak (AIME, Warrendale, PA, 1986) p. 155.
30. C. P. YOU, A. W. THOMPSON and I. M. BERNSTIEN, *Scripta Metall.* **21** (1987) 181.
31. J. SHANG and R. O. RITCHIE, *Mater. Sci. Engng* **102** (1988) 181.

Received 24 October 1989
and accepted 24 April 1990